Chapter 13
Characterizing Walking Loads based on Force Measurements on Lightweight Pedestrian Bridges

Ghaffarian Dallali Elyar and Dey Pampa

Abstract With the increasing use of high-strength and lightweight materials in sustainable constructions, vibration serviceability often becomes the governing design criteria, particularly for pedestrian bridges subjected to human-induced walking excitations. For assessing the vibration serviceability of lightweight pedestrian bridges, characterizing the walking-induced ground reaction forces (GRFs), is crucial. While most of the existing walking load models are based on direct GRF measurements on rigid surfaces such as force plates or treadmills, there exists very limited studies based on direct force measurements on pedestrian bridges, that can represent real walking behaviour including the human-structure interactions (HSI) due to the vibrating surface of the structure. This study characterizes vertical GRFs induced by a single pedestrian, using force measurements collected at the support level of a lightweight aluminum pedestrian bridge with distinct vibration characteristics. We introduce a new probabilistic framework for estimating GRF values to simulate walking loads from a single pedestrian. By utilizing both time and frequency domain analyses, the proposed approach simultaneously accounts for HSI and uncertainties in walking activities. Future work will be expanded to groups of pedestrians, where interaction effects are expected to be more pronounced.

Keywords Human-structure Interaction · Lightweight Pedestrian Bridges · Ground Reaction Force · Human Induced Vibrations

Introduction

Given the increasing demands for architectural designs—particularly regarding length, slenderness, and the use of innovative lightweight materials—many new pedestrian structures are experiencing excessive vibrations, which can lead to discomfort for pedestrians. Current methods for analyzing human-induced vibrations typically model the pedestrian as a force moving at a constant speed across the structure [1]. The time-history of this force, known as the ground reaction force (GRF) is usually represented as periodic load considering as a sum of up to certain numbers of Fourier harmonic components [2]. However, this approach has been shown to frequently overestimate structural responses, specially in the resonant scenario where the amplitude of the bridge response is significant [3]. Increasing evidence suggests that this overestimation is partly due to the mechanical interaction between the structure and the pedestrian, known as the human-structure interaction (HSI) effect. This effect typically arises in structures with high levels of vibration [4]. Specifically, in terms of GRF, the HSI reduces the contact force exerted by the pedestrian on a vibrating structure compared to walking on a rigid surface [5].

There are several methods to estimate the GRF in the vertical direction, however, only a few effectively account for HSI which can significantly alter the GRF's shape and magnitude [6]. For example, methods using force plates assume a rigid surface, therefore, these methods are incapable of capturing interactional behavior between pedestrian(s) and bridge. On the other hand, the GRF can be also estimated via instrumented shoes or indirectly using bridge acceleration measurements that potentially can capture HSI on flexible structures; however, they may lack precision, with smoothing effects of pressure

Ghaffarian Dallali Elyar
PhD student, Civil and Water Engineering
e-mail: elyar.ghaffarian

Dey Pampa
Associate Professor, Civil and Water Engineering, Laval University, Quebec City, QC, Canada G1V 0A6
e-mail: pampa.dey@gci.ulaval.ca

Matthew Whelan et al. (eds.), *Dynamics of Civil Structures, Vol. 2*, Conference Proceedings
of the Society for Experimental Mechanics Series, https://doi.org/10.13052/97887-438-0147-4_13

integration in instrumented shoes and complexity of calculations in indirect method [7] and [8]. Attaching force plates to a vibrating bridge is a more recent approach, but it introduces potential errors due to frequency and phase mismatches between the bridge and the force plates [5]. Additionally, three-dimensional recordings using inertial measurement units can be compromised by "tissue artifacts," caused by relative movement between body segments, reducing the accuracy of GRF estimation [9]. Among the various methods, using load cells at the bridge support level is distinctive because it can account for HSI effects without influencing pedestrian behavior, as it does not require additional equipment on the pedestrian or complex calculations. However, analyzing the GRF components measured through load cells in resonant and near-resonant scenarios can be challenging due to the overlaps of bridge's energy with the harmonics of pedestrian walking.

Despite the semi-periodic nature of walking mechanisms, walking is assumed to be perfectly periodic in current design practices which recommends deterministic values of the dynamic load factors (DLFs) to estimate the GRF. Such assumption ignores the inherent uncertainties and random behavior of walking [7]. Consequently, there is an inherent bias in the DLF values, as they often represent only a single footfall, which does not encompass the full variability of walking forces at a given frequency. Nevertheless, a probabilistic approach, which accounts for uncertainties in walking behavior, could provide a more realistic and accurate model, though it has received limited attention in the literature and code provisions[10], [9], [11], [12], and [13].

Given these challenges, this study introduces a novel probabilistic framework that quantifies dynamic load factors (DLF) up to the 5^{th} harmonic of walking load, offering a more precise representation of walking-induced loads while accounting for HSI. This framework derives the probability density functions (PDFs) for each DLF value based on force measurements collected at the supports of a lightweight aluminum pedestrian bridge. The estimated DLF values accounts for the inherent variability in pedestrian walking patterns, as well as uncertainties introduced by the HSI effects.

Background

In the deterministic framework, it is assumed that the successive footfalls are identical and thus, the vertical force induced by walking pedestrian is represented by a Fourier series as follows [2]:

$$G_{(t)}=G+\sum_{i=1}^{n} G\alpha_i \sin(i2\pi f_p t+\Phi_i) \tag{1}$$

where, G is the pedestrian's weight in [N], α_i is the dynamic load factor corresponding to the i^{th} harmonic of the walking frequency, f_p is the pacing frequency of the pedestrian in [Hz], Φ_i is the phase shift of the i^{th} harmonic, and n is the number of contributing harmonics, respectively. Over the last few decades, extensive research has been dedicated to quantify the α_i values based on direct or indirect measurements of walking forces [14].

Traditionally, α_i values for each harmonic of the walking load are calculated by extracting the maximum values from the Fast Fourier Transform (FFT) response, known as the peak picking method [7]. However, as mentioned earlier, walking is a semi-periodic activity with significant uncertainties. These uncertainties, combined with the effects of HSI, can cause energy leakage into neighboring frequencies. As a result, a narrow-band stochastic representation of the GRF provides a more accurate quantification. This implies that a single α_i value may not accurately represent complex walking and associated GRF [7]. To address this, Peters et al. [7] introduced the time-domain averaging method. In this approach, instead of proposing a constant value associated with each integer of the walking load, contribution of the frequency bands around the integers of the walking load is taken into account. By band-pass filtering each harmonic within its associated frequency range and converting the signal back to the time domain, the average of the peak values is calculated, representing the $\alpha_i$value for that harmonic. This method called time domain averaging accounts for the uncertainties in walking load, including HSI and the semi-periodic nature of human locomotion. However, it has only been applied to GRF data collected from instrumented treadmills, which are not capable of capturing the natural walking of a pedestrian or the HSI effects due to the vibrating surface of the bridge [7].

Several models are available in the literature for calculating the vibration response of pedestrian bridges to the GRF induced by pedestrians [15]. One widely used approach is the moving force (MF) model, which simplifies the pedestrian and their load as a concentrated force moving along the bridge at a constant velocity, v [1], as shown in Figure 1. This method is also adopted by the current design standards for its simplicity and ease of calculation [16], [17], and [18]. However, this model lacks accuracy, particularly in resonant scenarios where the effects of HSI is significant [1]. Nevertheless, there is ongoing debate in the literature about whether the effects of HSI can be accounted for by adjusting the GRF shape and values, without resorting to complex interaction models for incorporating HSI into the bridge's response estimation [19].

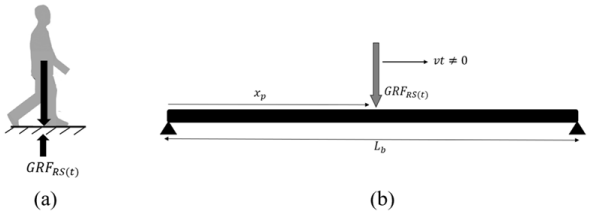

Fig. 1 (a) Ground reaction force exerted by a walking pedestrian (b) Moving force (MF) model on an equivalent beam.

Analysis

Experimental data

This study is based on the experimental study that was performed at the University of Waterloo (Canada) on a 22.9 m aluminum pony truss pedestrian bridge with a natural frequency of 4.58 Hz, total mass of 1735 Kg and modal damping of 0.8% [20]. More details of the tests can be found in [21] and [22]. During the experimental study, the bridge was instrumented with 4 triaxial load cells at four corner supports of the bridge to measure force time histories. 12 uniaxial accelerometers were also installed to measure vertical and lateral accelerations at both side of the bridge span (L) at L/4, L/2 and 3L/4 points. Numerous walking tests based on individual, and groups of pedestrians were conducted. In order to estimate the pedestrian-induced walking loads and validate them, this study is limited to the load cell data as well as the acceleration data at the middle of the bridge for a test subject representing a pedestrian with mass of 70 kg. During the walking tests, the test subject walked in five different pacing frequencies ranging from 1.67 Hz to 2.33 Hz with an interval of 0.167 Hz. This frequency range represents non-resonant, near-resonant, and resonant scenarios ensuring comprehensive coverage of different vibration-response conditions as classified in Table 1. In addition, each walking test for each frequency was repeated 30 times to account for the intra-subject variabilities. Figure 2 (a) illustrates the schematic layout of the pedestrian bridge, highlighting the positions of the load cells and accelerometer at the mid span. Additionally, Figures 2 (b) and 3 (c) present the force signals recorded from each load cell during an example trial, along with the total force, which is the sum of these signals, representing the pedestrian's impact and the resulting bridge vibrations.

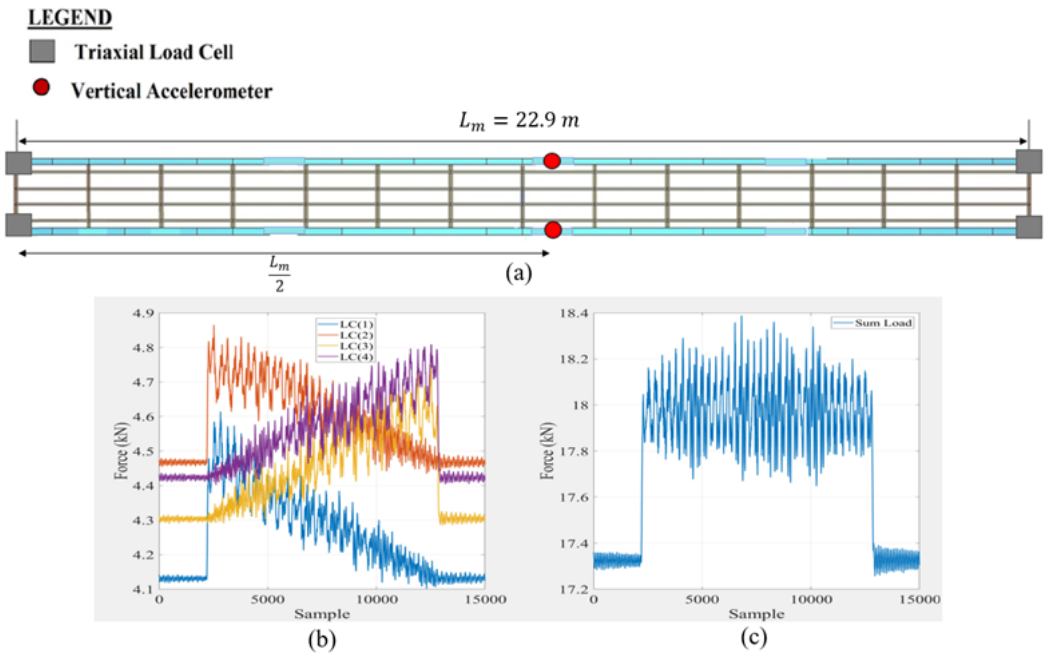

Fig. 2 (a) Schematic of the pedestrian bridge (modified from [17]); (b) raw force signals collected from load cells in the vertical direction; (c) Total force in vertical direction including all load cells.

Table 1 Classification of non-resonant, near resonant, and resonant scenarios based on the five pacing frequencies.

Pacing frequency	$f_p = (1.67)\,Hz$	$f_p = (1.83)\,Hz$	$f_p = (2.00)\,Hz$	$f_p = (2.17)\,Hz$	$f_p = (2.33)\,Hz$
Scenarios	NR-(H3)[2]	Non-resonant	Non-resonant	NR-(H2)[3]	R-(H2)[4]

f_p[1]: Pacing frequency of the pedestrian;
NR-(H3)[2]: near resonance with harmonic 3^{rd} harmonic of walking load.
R-(H2)[3]: near resonance with harmonic 2^{nd} harmonic of walking load.
R-(H2)[4]: resonance with harmonic 2^{nd} harmonic of walking load.

Estimation of DLF (α_i) values

In this section, the effects of uncertainty and HSI on the DLF values rre examined separately. In the first subsection, the DLF values for non-resonant scenarios are evaluated using both the peak picking and time-domain averaging methods. Since the bridge's acceleration response is low in these scenarios, the accuracy of each method can be attributed primarily to the uncertainties in the walking activity itself. In the second subsection, the DLF values for resonant and near-resonant scenarios are introduced using a probabilistic approach, which accounts for both the effects of HSI and the uncertainties in the GRF induced by pedestrians.

Non-resonant scenarios

In this section, the DLF values representing the GRF are calculated using both the traditional peak picking [23] and time-domain averaging methods [7], up to the 5^{th} harmonic of the walking load, based on data extracted from load cells. These values correspond to non-resonant scenarios (i.e.,$f_p = 1.83$ and 2.00 Hz). The mean DLF values on each method, considering all trials, are presented in Table 2. To evaluate the effectiveness of these DLF extraction methods, the maximum acceleration response of the bridge at mid-span is simulated using the MF modeling approach, incorporating the estimated DLF values. To do so, the bridge is represented as an equivalent single-degree-of-freedom (SDOF) system based on its mode of vibration with frequency of 4.58 Hz and damping of 0.8%. In the Figure 3, the simulated acceleration response is compared with the measured acceleration of the bridge at mid span. The maximum acceleration response is also simulated through the existing DLF values as proposed in the literature [17], [24], and [7], considering both pacing frequencies associated with non resonant state.

Table 2 Extracted DLF values for the first 5 harmonics of walking load using both peak picking and time domain averaging scenarios

	Frequency	α_1	α_2	α_3	α_4	α_5
Pick Picking	1.67	0.2441	0.0357	0.0607	0.0203	0.0062
	1.83	0.3416	0.1011	0.0532	0.0174	0.0060
Time Domain Averaging	2.00	0.2619	0.0553	0.0777	0.0253	0.0089
	2.17	0.3576	0.1190	0.0466	0.0208	0.0079

Using equation (2), the relative maximum acceleration response of the pedestrian bridge considering two current methodologies as well as the proposed values by two authors and CSA S7 is calculated. As evident from Table 3, the average relative maximum acceleration calculated using the DLF values extracted from load cell data via time-domain averaging provides the closest match between experimental observations and numerical results in the non-resonant scenarios. It is important to note that, in non-resonant conditions, the bridge's acceleration levels are relatively low, meaning the effects of HSI are less pronounced. Therefore, the accuracy of time-domain averaging in predicting the bridge response is likely not due to HSI effects on GRF values but rather to its ability to capture the uncertainties in natural walking behavior using load cell data. In contrast, the inaccuracy of the peak picking method supports the hypothesis that human walking activity resembles a narrow-banded stochastic signal, which cannot be accurately represented by fixed α_i values. Therefore, this conclusion can be drawn that the uncertainties in walking behavior causes energy leakage into neighboring frequencies, while the amplitude of these neighbor frequencies might not be prominent in the frequency domain, still contribute to the accuracy of pedestrian-induced walking load prediction.

$$\beta = \left(\frac{a_{num} - a_{exp}}{a_{exp}} * 100 \right) \tag{2}$$

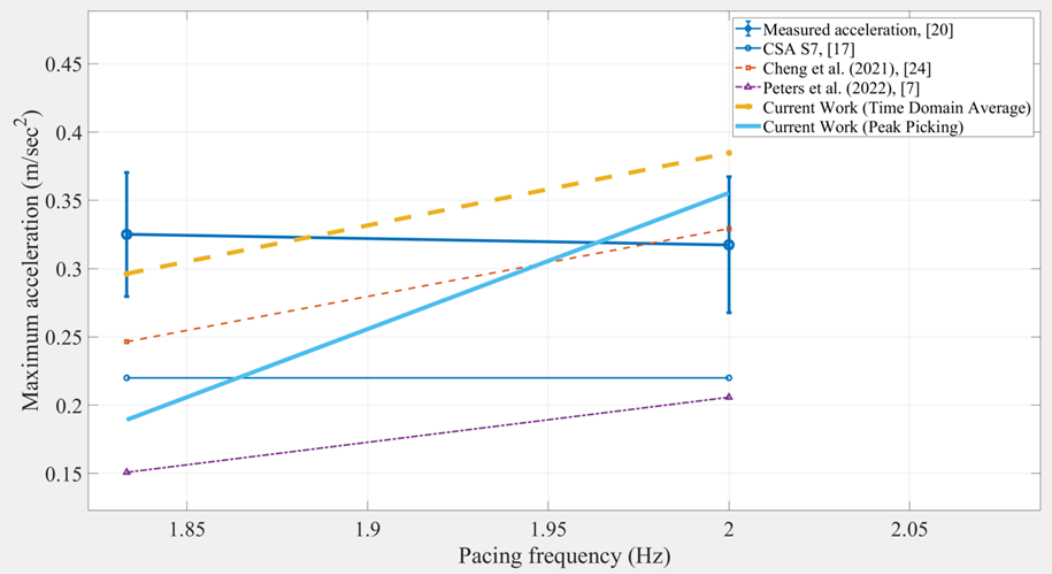

Fig. 3 Comparisons of the measured maximum accelerations at the mid span of the bridge with the simulated ones using the DLF values extracted from two methods as well as proposed in the literature [20], [17], [24], and [7].

Table 3 Relative acceleration response of the bridge using peak picking and time domain averaging as well as the relative simulated response of the bridge using DLF values introduced by two other authors and CSA S7.

	$\beta_{f_{1.83}}$	$\beta_{f_{2.00}}$	$\frac{\beta_{f_{1.83}}+\beta_{f_{2.00}}}{2}$
CSA S7 [16]	-32.30	-30.59	-31.45
Chen et al. [22]	-24.30	3.78	-10.26
Peters et al. [7]	-53.84	-35.33	-44.58
Current Work (Peak Picking)	-41.84	11.98	-14.92
Current Work (Time Domain Averaging)	-8.92	21.13	6.10

Resonant and near-resonant scenarios

In this subsection, an improved DLF estimation framework is proposed for both the resonant and near-resonant scenarios that combines a modified time domain averaging method to the approach proposed by Ahmadi et al. [5] for separating bridge contributions from the force signals based on synchronized force and acceleration signals measured on the bridge. It should be noted that the DLF value corresponding to the resonant harmonic is only determined for resonant scenarios, as it absorbs the highest energy in the system, with negligible contributions from other harmonics.

Since the acceleration at the middle of the bridge and the force signals at the supports as collected by Dey et al. [22] were not synchronized due to the use of different acquisition systems, the first step of this approach involves synchronizing the force and acceleration signals using cross-correlation technique [25]. The next step involves calculating the mean inertial mass of the bridge by dividing the force signal by the synchronized acceleration response at the center of the bridge during the decay phase of vibration, i.e., when the pedestrian has left the bridge, and it vibrates freely without external forces. The inertial mass of the bridge was estimated to be 1082 kg, which is slightly higher than half of the total bridge mass, a result consistent with modeling the bridge as an equivalent simply supported beam. Next, both the force signal from the load cell and the acceleration response are filtered using a band-pass filter to isolate the frequency band of the resonant or near-resonant harmonic during the forced phase of vibration, while the pedestrian is still on the bridge. The filtered acceleration during this phase is then multiplied by the previously calculated inertial mass, representing the bridge's modal force in the selected frequency band where the harmonic of the walking load and the bridge's modal response overlap. Finally, by subtracting the load cell data during the forced phase from the calculated modal force, the force values associated with the resonant or near-resonant harmonics can be obtained, without the contribution of the bridge's modal response. Once the force signals are extracted, a modified time-domain approach as described in Figure 4 is applied to determine the DLF values. The traditional Time Domain Averaging proposed by Peters et al. [7] used the mean values of the signal peaks (as indicated by

green line in Figure 4) in the time domain to propose DLF values associated with each harmonic of walking load. In this study, instead of using mean peak value, all the peaks of the force signals (as shown in red dots in Figure 4), associated with a specific frequency band corresponding to a walking harmonic, is extracted. All these peaks for all walking trials are then presented in a probabilistic framework as discussed in the next section.

Fig. 4 Modified approach to extract DLF through Time Domain Averaging method.

Statistical distribution of estimated DLF values

Once the DLF values for each walking trial and each frequency are calculated, the statistical distribution of the DLF values are determined. It should be noted that similar to the resonant and near-resonant cases, the modified time domain averaging method is also applied to extract each peak of the GRF signals corresponding to a harmonic which are then modelled probabilistically including all walking trials. It has been observed that in case of non-resonant scenarios, only the first harmonic of walking load follows a specific statistical distribution. Hence, the α_1 is presented within a probabilistic framework, while the mean DLF values are reported for the remaining harmonics. Similarly, in the near-resonant scenarios, a statistical distribution is introduced for both the first and resonant harmonics, with mean values presented for the remaining harmonics. Finally, in the resonant scenario, the statistical distribution and PDF are provided only for the resonant harmonic, as it absorbs the highest energy in the system, with negligible contributions from other harmonics.

To identify the most suitable probability density function (PDF) for representing the DLF values, the Akaike Information Criterion (AIC) was applied to various statistical distributions. The results indicated that the t-distribution, characterized by its three parameters—location (μ), scale (σ), and degrees of freedom (ν)—provided the best fit for all PDFs. For instance, Figure 5 illustrates the PDF for the second harmonic of the walking load in a resonant situation with a pacing frequency of 2.17 Hz. Additionally, Table 3 summarizes the mean DLF values for harmonics that do not require a PDF representation, while Table 4 presents the PDF parameters for all pacing frequencies.

Table 4 Mean DLF values for non-resonant scenarios for 5 harmonics and different pacing frequencies.

Frequency (Hz)	α_1	α_2	α_3	α_4	α_5
1.67	t-student	0.1190	t-student	0.0208	0.0079
1.83	t-student	0.0553	0.0777	0.0254	0.0089
2.00	t-student	0.1190	0.0466	0.0208	0.0079
2.17	t-student	t-student	0.0297	0.0231	0.0185
2.33	0	t-student	0	0	0

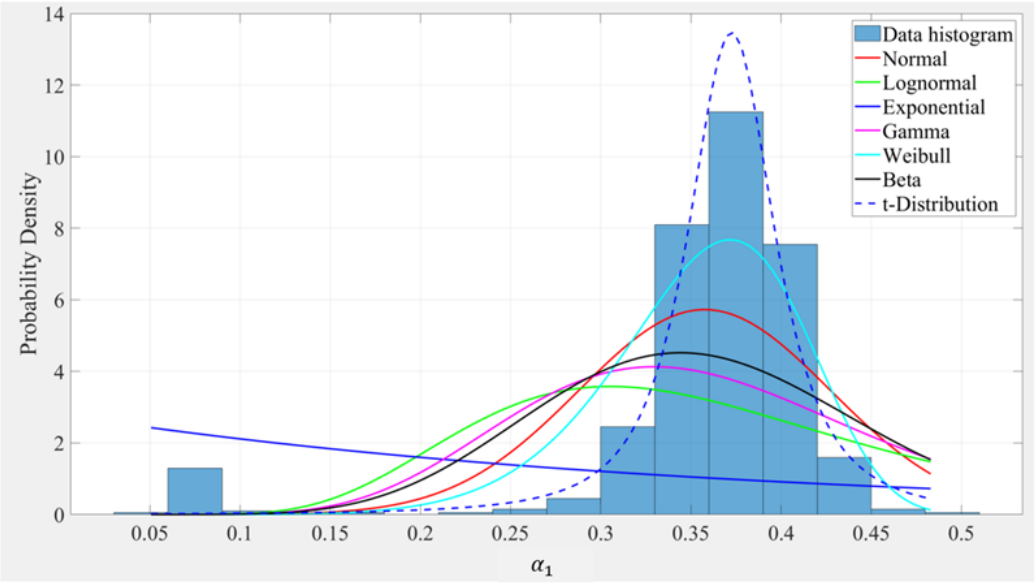

Fig. 5 Different PDFs of the first DLF value for pacing frequency equal to 2.17 Hz.

Table 5 t-student parameters for DLF values of resonant and near resonant scenarios considering all pacing frequencies

Frequency (Hz)	α_i	μ	σ	ν
1.67	α_1	0.2522	0.0162	1.7398
	α_3	0.0324	0.009	12.0619
1.83	α_1	0.2728	0.0189	1.732
2.00	α_1	0.3725	0.0261	1.9506
2.17	α_1	0.4154	0.0446	1.6941
	α_2	0.0392	0.0129	4491372.8
2.33	α_2	0.0597	0.0188	763697.6

Comparison of maximum responses in a probabilistic framework

This section assesses the performance of the estimated DLF values and their statistical distributions to simulate bridge response probabilistically. Based on the 30 walking trials during the experimental study, the histogram of the measured acceleration is plotted in Figure 6. For the predicted response based on the estimated DLF values, a total of 6000 simulations were performed using Monte Carlo simulation and are presented in Figure 6 to compare and assess its performance with respect to the experimental measurements.

As shown in Figure 6, there is strong agreement between the simulated and experimental results. However, for non-resonant scenarios ($f_p = 1.83$ and 2.00 Hz), the maximum acceleration response of the bridge is more widely distributed. This suggests that when the excitation energy is not concentrated in a specific frequency range, the coupled bridge-pedestrian system exhibits more scattered responses. This could also indicate a higher level of uncertainty in the pedestrian's walking activity in non-resonant scenarios, as the pedestrian is not synchronizing their steps with the bridge's vibrations, leading to varying and scattered output in each trial. Conversely, in resonant and near-resonant scenarios, the maximum response of the bridge is more concentrated. This could be attributed to the stronger effects of HSI and to the fact that the pedestrian is more inclined to modify their steps with respect to the oscillatory surface. Moreover, for the resonant scenario ($f_p = 2.33$ Hz), there is a good agreement between the experimental and simulated responses. However, in near-resonant scenarios, the predictions slightly underestimate the system's response. This discrepancy could be due to inaccuracies in the method developed by Ahmadi et al. for near-resonant conditions or unique dynamic characteristics of lightweight aluminum bridges However, further investigation is required to understand why the DLF values extracted from the same bridge in near-resonant conditions underestimate the system response.

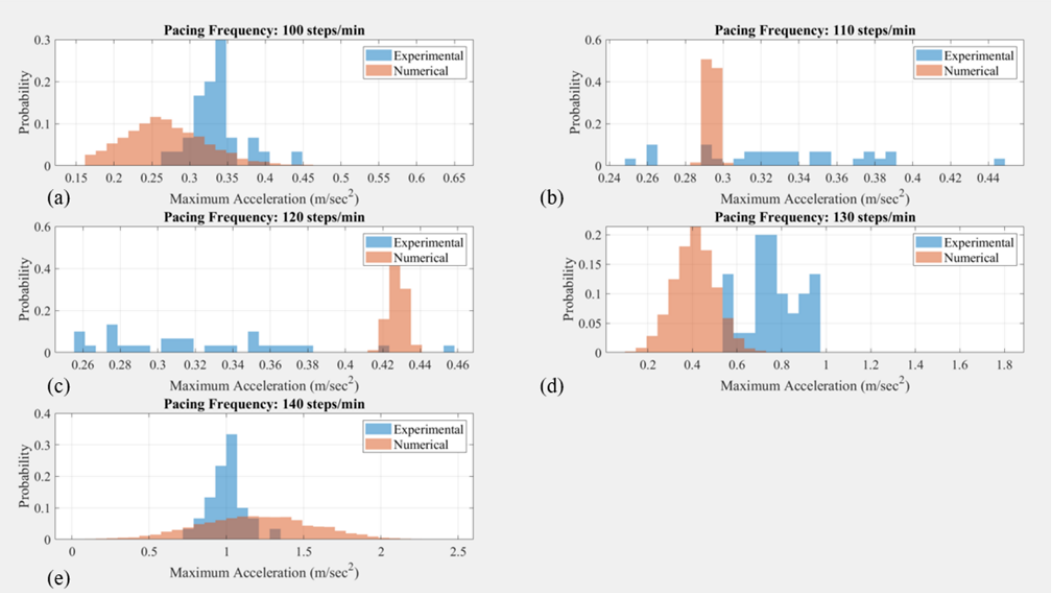

Fig. 6 Probability distributions of simulated and measured acceleration responses for a) $f_p = 1.67$ Hz, b) $f_p = 1.83$ Hz, c) $f_p = 2.00$ Hz, d) $f_p = 2.17$ Hz, and e) $f_p = 2.33$ Hz.

Conclusion

In this study, the ground reaction force (GRF) induced by a single pedestrian was estimated using force signals from load cells, applying a hybrid time-frequency domain representation of the force and estimating the dynamic load factor (DLF) values in a probabilistic framework. In the first part of the analysis, two methodologies—peak picking and time domain averaging—were evaluated by calculating the maximum acceleration response of the bridge in non-resonant scenarios. It is concluded that the time domain averaging technique captured the uncertainties in walking loads more effectively, suggesting it may be a better method for developing GRF values compared to the peak picking approach. An improved method is also proposed to estimate DLF values for resonant and near-resonant harmonics. Finally, all the DLF values for resonant, near-resonant, and non-resonant scenarios are determined probabilistically. The analysis showed that for all scenarios, the first DLF, near-resonant, and resonant harmonics were best described by the t-distribution, while the remaining harmonics were represented by their mean values, as they did not follow a specific statistical distribution. To further assess the performance of the extracted DLF values and their statistical distribution, the predicted maximum acceleration responses through Monte Carlo simulations are compared with the experimental observations. The results imply that the estimated maximum acceleration responses are in good agreement with the measured responses for resonant scenarios indicating better performance of the proposed framework. On the other hand, the experimental results were more scattered as compared to the predicted ones for non-resonant scenarios, implying higher uncertainty in these situations. In fact, during resonant scenarios, since pedestrians tend to synchronize their steps to the bridge oscillations, the uncertainty in walking becomes lower, yielding in narrow band representations of the bridge responses as compared to non-resonant scenarios. Additionally, in near-resonant scenarios, although DLF values were estimated for both resonant and non-resonant harmonics, the proposed methodology underestimates the bridge response, which could be due to the limitations of the DLF extraction method or specific dynamic characteristics of lightweight bridge in near-resonant conditions. However, further study is needed to investigate the near-resonant scenarios. In the future scope of this study, the proposed framework will be extended to groups of pedestrians.

Acknowledgments The research presented in this paper was financially supported by the Natural Sciences and Engineering Research Council of Canada (NSERC) through the Discovery Grant program, and the Fonds de recherche du Québec – Nature et technologies (FRQNT). The authors gratefully acknowledge this support. The authors also acknowledge Prof. Scott Walbridge and Prof. Sriram Narasimhan who were the principal investigators for the previous research project on aluminum pedestrian bridges that funded the past experimental study led by the last author of this article.

References

1. C. C. Caprani and E. Ahmadi, "Formulation of human–structure interaction system models for vertical vibration", J. Sound Vib., vol. 377, pp. 346–367, 2016.
2. V. Racic, A. Pavic, and J. M. W. Brownjohn, "Experimental identification and analytical modelling of human walking forces: Literature review", J. Sound Vib., vol. 326, no. 1–2, pp. 1–49, 2009.
3. S. Živanović, A. Pavic, and P. Reynolds, "Vibration serviceability of footbridges under human-induced excitation: a literature review", J. Sound Vib., vol. 279, no. 1–2, pp. 1–74, 2005.
4. A. Firus, J. Schneider, H. Berthold, M. Albinger, and A. Seyfarth, "Parameter identification of a biodynamic walking model for human-strncture interaction", in Maintenance, Safety, Risk, Management and Life-Cycle Performance of Bridges, CRC Press, 2018, pp. 668–674. Accessed: Sep. 20, 2024. [Online]. Available: https://www.taylorfrancis.com/chapters/edit/10.1201/9781315189390-90/parameter-identification-biodynamic-walking-model-human-strncture-interaction-firus-schneider-berthold-albinger-seyfarth
5. E. Ahmadi, C. Caprani, S. Živanović, and A. Heidarpour, "Vertical ground reaction forces on rigid and vibrating surfaces for vibration serviceability assessment of structures", Eng. Struct., vol. 172, pp. 723–738, 2018.
6. V. Racic, A. Pavic, and J. M. W. Brownjohn, "Modern facilities for experimental measurement of dynamic loads induced by humans: A literature review", Shock Vib., vol. 20, no. 1, pp. 53–67, 2013.
7. A. E. Peters, V. Racic, S. Živanović, and J. Orr, "Fourier series approximation of vertical walking force-time history through frequentist and Bayesian inference", Vibration, vol. 5, no. 4, pp. 883–913, 2022.
8. A. Firus, R. Kemmler, H. Berthold, S. Lorenzen, and J. Schneider, "A time domain method for reconstruction of pedestrian induced loads on vibrating structures", Mech. Syst. Signal Process., vol. 171, p. 108887, 2022.
9. M. Zhang, C. T. Georgakis, and J. Chen, "Biomechanically excited SMD model of a walking pedestrian", J. Bridge Eng., vol. 21, no. 8, p. C4016003, 2016.
10. H. Wang, J. Chen, and J. M. Brownjohn, "Parameter identification of pedestrian's spring-mass-damper model by ground reaction force records through a particle filter approach", J. Sound Vib., vol. 411, pp. 409–421, 2017.
11. W. E. Saul, C. Y.-B. Tuan, and B. McDonald, "Loads due to human movements", in Structural Safety Studies, ASCE, 1985, pp. 107–119.
12. C. Y. Tuan and W. E. Saul, "Loads due to spectator movements", J. Struct. Eng., vol. 111, no. 2, pp. 418–434, 1985.
13. P. Dey, S. Walbridge, and S. Narasimhan, "Evaluation of design provisions for pedestrian bridges using a structural reliability framework", J. Bridge Eng., vol. 23, no. 2, p. 04017132, 2018.
14. Z. O. Muhammad and P. Reynolds, "Vibration Serviceability of Building Floors: Performance Evaluation of Contemporary Design Guidelines", J. Perform. Constr. Facil., vol. 33, no. 2, p. 04019012, Apr. 2019, doi:10.1061/(ASCE)CF.1943-5509.0001280.
15. E. Shahabpoor, A. Pavic, and V. Racic, "Interaction between walking humans and structures in vertical direction: A literature review", Shock Vib., vol. 2016, 2016.
16. P. Charles and W. Hoorpah, "Technical Guide: Footbridges–Assessment of vibrational behaviour of footbridges under pedestrian loading", Paris SetraAFGC, 2006.
17. CSA(National Standard of Canada). (2023). "Pedestrian, cycling, and multiuse bridge design guideline."CAN/CSA S7-23, ON, Canada.
18. C. C. Code, "CAN/CSA S6-06", Can. Stand. Assoc. Can., vol. 734, 2006, Accessed: May 13, 2024. [Online]. Available: https://www.multibriefs.com/briefs/csce/S17_2014_Fredericton.pdf
19. E. Ahmadi, C. Caprani, S. Živanović, N. Evans, and A. Heidarpour, "A framework for quantification of human-structure interaction in vertical direction", J. Sound Vib., vol. 432, pp. 351–372, 2018.
20. P. Dey, S. Narasimhan, and S. Walbridge, "Evaluation of design guidelines for the serviceability assessment of aluminum pedestrian bridges", J. Bridge Eng., vol. 22, no. 1, p. 04016109, 2017.
21. P. Dey, "Evaluation and Calibration of Pedestrian Bridge Standards for Vibration Serviceability", 2017.
22. P. Dey, A. Sychterz, S. Narasimhan, and S. Walbridge, "Performance of pedestrian-load models through experimental studies on lightweight aluminum bridges", J. Bridge Eng., vol. 21, no. 8, p. C4015005, 2016.
23. J. Blanchard, B. L. Davies, and J. W. Smith, "Design criteria and analysis for dynamic loading of footbridges", in Proceeding of a Symposium on Dynamic Behaviour of Bridges at the Transport and Road Research Laboratory, Crowthorne, Berkshire, England, May 19, 1977., 1977.
24. J. Chen, P. Wang, and H. Wang, "Pedestrian-Induced Load Identification from Structural Responses Using Genetic Algorithm with Numerical and Experimental Validation", J. Bridge Eng., vol. 26, no. 3, p. 04021001, Mar. 2021, doi:10.1061/(ASCE)BE.1943-5592.0001687.
25. A. V. Oppenheim, "AS Willsky, and SH Nawab", Signals Syst., 1996.